NASA TN D-396

7N-39
198982
P-35

TECHNICAL NOTE

D-396

SOME EXPERIMENTS CONCERNING SUBSEQUENT YIELD SURFACES

IN PLASTICITY

By Harvey G. McComb, Jr.

Langley Research Center
Langley Field, Va.

NATIONAL AERONAUTICS AND SPACE ADMINISTRATION

WASHINGTON June 1960

(NASA-TN-D-396) SOME EXPERIMENTS CONCERNING SUBSEQUENT YIELD SURFACES IN PLASTICITY (NASA. Langley Research Center) 35 p

N89-71014

Unclas
00/39 0198982

1N

NATIONAL AERONAUTICS AND SPACE ADMINISTRATION

TECHNICAL NOTE D-396

SOME EXPERIMENTS CONCERNING SUBSEQUENT YIELD SURFACES IN PLASTICITY

By Harvey G. McComb, Jr.

SUMMARY

Some experiments to obtain further knowledge concerning subsequent yield surfaces in plasticity have been performed. Combined load tests have been made on seven thin-walled tube specimens of 2014-T4 aluminum alloy. The secondary (that is, the first subsequent) yield surface is outlined in the normal-stress—shear-stress plane for an initial loading in pure tension. Discussion is presented of significant changes in the shape of the stress-strain curves obtained from the tests of the thin-walled tube specimens.

INTRODUCTION

The plastic behavior of strain-hardening metals under combined loading is considerably more complicated than their behavior under uniaxial loading. The term "yield point" or "elastic limit" is often applied to the boundary between the elastic and plastic states under uniaxial loading. Under combined loading, on the other hand, the yield point is generalized into a yield surface to represent the boundary in stress space between elastic and plastic states. In the uniaxial loading case, initial loading beyond the yield point in tension, for example, establishes new yield points in both tension and compression for a subsequent loading. The term "Bauschinger effect" is used in this report to denote the unequal raising or the lowering of the yield point upon the reversal of a uniaxial stress or a state of pure shear stress.

Changes in the yield point due to uniaxial loadings beyond the elastic range are well established for many materials. Very little is known, however, about changes in the shape of the yield surface. Various theories of plasticity predict widely different changes in the yield surface due to loading. For instance, the simple incremental theory of plasticity, based on the Von Mises yield criterion (simple J_2 flow theory, see ref. 1), predicts a smooth yield surface which

expands uniformly upon loading. According to this theory, successive yield surfaces form a "nested" set of surfaces having a common center. Figure 1(a) illustrates this situation for a two-dimensional stress space. Figure 1(b) illustrates the change in the yield surface in a two-dimensional space predicted by another theory, the slip theory of Batdorf and Budiansky. (See ref. 2.) According to this theory, a "corner" is formed in the yield surface due to loading and a significant portion of the initial yield surface may remain undistorted.

Experimental data to aid in the development or refinement of theory are sparse. In reference 3 the secondary (that is, the first subsequent) yield surface in the normal-stress—shear-stress plane for 2024-T4 aluminum alloy was investigated. A number of thin-walled tubes were tested in combined tension and torsion in order to outline the yield surface resulting from an initial loading in pure torsion. A pronounced Bauschinger effect was noted when a specimen was loaded in pure torsion, unloaded, and then reloaded in reversed torsion. The yield surface in the vicinity of pure tension, on the other hand, was not affected by the initial loading in torsion.

L
7
6
9

Numerous investigations into the occurrence of corners in the yield surface have led to results that have been somewhat conflicting. However, the results reported in references 4 and 5 concerning combined tension-torsion tests made on thin-walled tubes of commercially pure aluminum strongly indicate that corners do appear, but the angle included by the corner approaches 180°.

The present investigation is intended as a further contribution to the experimental knowledge of changes in the yield surface caused by loading. In these tests seven thin-walled tubes of 2014-T4 aluminum alloy were loaded in various combinations of tension or compression and torsion. The loading paths were the simplest possible combined loadings; that is, the normal stress and shear stress were maintained proportional throughout the loading. Such paths are called proportional or radial loading paths. All specimens except one were initially loaded into the plastic range in pure tension. After removal of the initial load, various combined loadings were applied and removed, and stress-strain curves were obtained from these combined loadings. In this report, some interesting features concerning the shape of these stress-strain curves are discussed. Also, there is shown the secondary yield surface in the normal-stress—shear-stress plane established by an initial loading in pure tension.

SYMBOLS

f	functional relation between plastic strain and stress for standard stress-strain curve
J_2	second invariant of stress deviation tensor
γ_p	plastic portion of shear strain
ϵ	normal strain
ϵ_p	plastic portion of normal strain
λ	constant defined by equation $\epsilon_p = f(\lambda\sigma)$
σ	normal stress
σ_s	normal stress associated with standard stress-strain curve
σ_y	normal stress at yield point
τ	shear stress

L
7
6
9

SPECIMENS AND EQUIPMENT

Specimens

The specimens tested in this investigation were thin-walled cylinders or tubes. This configuration is useful because axial and torsional loadings provide essentially two-dimensional states of stress and strain in the specimen. The wall thickness of the specimens was chosen small enough to produce negligible stress variation through the thickness and yet sufficiently large to prevent buckling within the range of compressive and torsional loads which were to be applied. The specimens for this investigation were machined from commercially forged 2014-T61 aluminum-alloy stock. This stock was in the form of cylindrical billets 10 inches in diameter and approximately 6 feet long. The billets were cut into 2-foot lengths and rough-machined to $7\frac{3}{4}$ inches in diameter. These 2-foot-long cylinders were then reheattreated to the -T4 temper before the boring and final machining operations were carried out.

The nominal dimensions of the specimens are shown in figure 2 and were the same as those tested in the investigation of reference 6. The specimens had a nominal outside diameter of 4.5 inches, a nominal thickness of 0.156 inch, and a nominal length of 24 inches. The test section

of each specimen was a constant section approximately 12 inches long at the center of the specimen. (See fig. 2.) The outside diameter and wall thickness were checked on each specimen at a number of locations throughout the test section. Variations from the average for a given specimen were small. For instance, the largest variation in outside diameter was 0.75 percent and the largest variation in thickness was 2.9 percent.

Equipment

L
7
6
9

The tests on the thin-walled tube specimens were carried out in the combined load testing machine of the Langley structures research laboratory. Figure 3 shows the testing machine with a specimen mounted between the loading head on the left and the weighing head on the right. This testing machine is hydraulically operated and is capable of applying and measuring six load components - axial, torsional, bending in two perpendicular planes, and shear in two perpendicular directions. Only the axial and torsional load components of the testing machine were utilized in applying loads to the specimens in these tests; the remaining components were monitored to insure that they remained small. An autographic recorder was used to record the loads and the output of the instruments mounted on the specimen.

Strain measurements were made with electrical-resistance strain rosettes and with specially designed twist gages and extensometers. Two twist gages and two extensometers were mounted on each thin-walled tube specimen. The twist gages were cantilever-beam devices having a 10-inch gage length and were mounted on the specimen as shown in figure 4. They were the same gages employed in the tests of reference 6. Twisting the specimen caused the cantilever beams to deflect, and electrical-resistance strain gages on the cantilevers were calibrated to read directly the shear strain in the specimen. In figure 5 the extensometers are shown mounted on the top and bottom of a specimen in the testing machine. Also shown in this figure is the top view of one twist gage. The extensometers were linear differential transformers attached to fixtures in such a way that one set of gage points moved with the coil and the other set moved with the core. The attachment between the core and its mounting fixture was a flexure device which allowed a small amount of lateral motion in order to prevent the core from binding in the coil when the test specimen was twisted. All strains reported herein are those measured by the twist gages and extensometers. The records from the electrical-resistance strain rosettes were used to check the twist gage and extensometer readings in the elastic range.

The accuracies of the load measuring and recording systems were estimated to be as follows: For axial load, ±450 pounds or ±1 percent

of the applied load; for torsional load, ±350 pound-inches or ±1 percent of the applied moment. The accuracies of the strain measuring and recording systems were equivalent to the following: For axial strain, ±100 microinches per inch; for shear strain, ±200 microinches per inch.

PRELIMINARY STRESS-STRAIN TESTS

L
7
6
9

For the purposes of this investigation, the yield point was defined to be the proportional limit. In order to provide a fairly consistent determination of the proportional limit for a pure tensile stress, some preliminary stress-strain tests were made on coupons with the use of Tuckerman optical strain gages. These coupons were machined from the same billets as the thin-walled tube specimens and alined with the longitudinal axis of the billet and the tube specimen. The coupons were obtained from slabs which were sawed off the sides of the 2014-T61 aluminum-alloy billets after they had been cut to 2-foot lengths but before rough-machining. The slabs were reheattreated to the -T4 temper at the same time as the rough-machined cylinders. Then the stress-strain coupons were machined from the slabs. The center lines of the coupons were approximately 1/2 inch from the original billet surface.

The stress-strain curves from the coupons showed some variation from one billet to another. It was found, however, that in the initial portion of the plastic range the various stress-strain curves could be correlated in the same way as discussed in reference 6. A "standard" curve was selected from among those obtained from the coupon tests, and comparisons were made between the other stress-strain curves and the standard curve. In order to make a comparison, the ratio $\lambda = \sigma_s/\sigma$ was calculated for various values of ϵ_p where, for a given value of ϵ_p, σ_s is the stress from the standard curve and σ is the stress from the other curve. For each comparison, the values of λ were practically independent of ϵ_p. In other words, the initial plastic portions of the stress-strain curves from the various billets could be approximated by $\epsilon_p = f(\lambda\sigma)$. Actually, values of λ were determined for each thin-walled tube specimen by comparing the stress-strain curve obtained from a test on the specimen in pure tension with the standard curve obtained from a test on a stress-strain coupon. The value of λ for each specimen is given in table I.

The Tuckerman gages on the stress-strain coupon provided a more precise and consistent value of yield point (proportional limit) than could be obtained from the extensometers and their recording system. This correlation between the specimens and the standard stress-strain

coupon is illustrated in figure 6. The points shown are from the experiments on specimens 2 and 7. The three curves presented are the standard curve and two curves calculated from the standard for $\lambda = 0.956$ and $\lambda = 1.051$. Data from all other thin-walled tube specimens gave values of λ between these two values, and comparisons between the experimental points and the calculated curves were as good as or better than those shown in figure 6. With this procedure the yield points (proportional limits) for the various tube specimens in pure tension were assumed to be given by $\sigma_y = 31.5$ ksi/λ, the value 31.5 ksi being the yield point of the standard stress-strain curve. The horizontal arrows in figure 6 indicate the yield points for the three curves shown.

L
7
6
9

The following are average results obtained from the stress-strain tests on the tensile coupons:

Proportional limit, ksi	30.0
Yield strength (0.2-percent offset), ksi	40.8
Ultimate tensile strength, ksi	64.3

In addition to the tensile tests, some compressive stress-strain tests were made on 1-inch by 1-inch by 3-inch coupons made from material removed from the holes in the thin-walled tube specimens. Results for the average 0.2-percent-offset yield strength were as follows: For longitudinal tests, 42.7 ksi; for transverse tests, 40.6 ksi. The lack of isotropy suggested by these results is probably about what can be expected in stock material of this kind.

TESTING TECHNIQUE

In these tests it was desired to load the thin-walled tube specimens in such a way as to determine the secondary yield surface in the σ,τ plane established by an initial pure-tensile load beyond the elastic range. Also, plastic strains were to be obtained for various subsequent radial loading paths to provide data which might be useful in the development of plasticity theory.

The loading programs which were applied to the various specimens are shown in table I. The ellipses shown in the sketches in table I represent the initial yield surface. The heavy radial lines represent the loading paths over which the specimens were loaded and then unloaded. Each radial line represents a run, that is, a complete cycle of loading and unloading. The numbers at the ends of the paths indicate the sequence of loading. Usually when one run was completed, the subsequent run was started immediately. For certain specimens, however, there was an elapse of approximately one day between run 1 and run 2

(specimens 2, 3, and 6), and in one case run 2 was not carried out until the third day after run 1 (specimen 5). Table I also contains the dates on which the various tests were carried out.

The specimens were loaded continuously in the hydraulically operated testing machine. Loads and strains were recorded continuously on an autographic recorder. The loads were applied at rates equivalent to strain rates of between 500 and 1,000 microinches per inch per minute. The heads of the testing machine were maintained approximately parallel during all tests. Occasionally small end moments and shears developed due to slight nonuniformities in the specimens, but strains in the test sections of the specimens were approximately homogeneous.

L
7
6
9

RESULTS

The secondary yield surface due to an initial pure-tensile load into the plastic range as determined by these tests is shown in figure 7. In figures 8 to 14 are shown stress—plastic-strain curves obtained from the various radial loadings. A sketch of the loading paths from table I corresponding to the specimen tested is repeated in these figures. The horizontal arrows adjacent to most of these curves indicate approximate values of the yield points. These yield points were obtained from data plots made to a considerably larger scale than in these figures.

Secondary Yield Surface

The dashed line in figure 7 shows the secondary yield surface in the σ,τ plane as determined by these tests. The coordinates in this figure are nondimensionalized with respect to σ_y, the yield-point stress in pure tension. This yield-point stress was obtained from the initial loading for specimens 1 to 6 and from the second loading for specimen 7. Point A represents the average of the maximum tensile stresses for the initial loading on specimens 1 to 6 and the second loading on specimen 7. These stresses were 32 percent ±2 above the various initial yield points in pure tension. Points B, C, D, E, and F were obtained from the second loading on specimens 2, 3, 4, 5, and 6, respectively, and represent the points at which the stress-strain curves obtained from these loadings departed from linearity; therefore, they are points on the secondary yield surface. Points G and H resulted from tests on specimen 7. Point G represents the yield point in pure shear obtained from the initial loading and based on σ_y obtained from the second loading. This point lies very nearly on the Tresca (maximum shear stress) ellipse. Point H represents the yield point obtained from the third loading (run 3) on specimen 7 (pure compression). If

the assumption is made that the initial pure-shear loading does not affect the yield point in tension or compression (as indicated in ref. 3), point H may be taken as a point on the secondary yield surface.

The following section presents a detailed description of the tests on the various thin-walled tube specimens. Also, some interesting changes in shape which appear in the resulting stress-strain curves are discussed.

Stress-Strain Curves From Thin-Walled Tube Specimens

L
7
6
9

Specimen 1.- The thin-walled tube specimen 1 was loaded only in pure tension. (See fig. 8.) The initial load produced an axial stress about 32 percent above the initial yield point. (This increase was also obtained for initial loads on all the remaining specimens except specimen 7.) The subsequent load on specimen 1, again in pure tension, produced a sharp bend in the stress-strain curve. The point of initial maximum tensile stress is thus established as a point approximately on the secondary yield surface.

Specimen 2.- The second loading on specimen 2 was in combined tension and torsion at a ratio $\sigma/\tau \approx 3$. (See fig. 9.) The σ,ϵ_p and τ,γ_p curves resulting from this loading give evidence of yielding much earlier than predicted by J_2 deformation or flow theories. The third loading, then, was along the same radial path as the second. Sharp bends are evident in both of the stress—plastic-strain curves of run 3. The fourth loading, in which the torsion is reversed ($\sigma/\tau \approx -3$), again produces a smooth stress-strain curve. The final loading (run 5) on this specimen was in pure tension again. It is seen that the resulting stress-strain curve exhibits significant yielding below the previously highest stress in pure tension; furthermore, the curve is smooth. Despite the fact that the three combined loadings subsequent to the initial tensile load were primarily in tension, these loadings (runs 2, 3, and 4) produced a significant reduction in the pure-tensile yield point established by the initial load.

Specimen 3.- The second loading on specimen 3 was in combined tension and torsion at a ratio $\sigma/\tau \approx 1$. (See fig. 10.) The third loading was in pure tension. The stress-strain curves for runs 2 and 3 are all smooth. The curve for run 3 exhibits significant yielding considerably below the initial maximum tensile stress. Runs 4 and 5 were at a ratio $\sigma/\tau \approx -1$ (torsion reversed). The curves from run 4 are smooth, but sharp bends appear in both the σ,ϵ_p and the τ,γ_p curves for run 5.

Specimen 4.- Specimen 4 was loaded in pure tension and in pure torsion. (See fig. 11.) Both runs 2 and 3 were in pure torsion. Run 3

exhibits the sharply bending stress-strain curve. Run 4 in which torsion is reversed shows a pronounced reduction in yield point compared with that obtained for run 2, and a smooth stress-strain curve results. The fifth loading in pure tension gives a smooth stress-strain curve which yields considerably below the initial maximum tensile stress. In fact, this loading indicates yielding well below the initial yield point.

Specimens 5 and 6.- Specimens 5 and 6 received second loadings in combined compression and torsion to indicate the shape of the yield surface to the left of the τ-axis in the σ,τ plane. The second loading on specimen 5 was at a ratio $\sigma/\tau \approx -1$. (See fig. 12.) The third loading on this specimen was in pure tension and produced a smooth stress-strain curve which yielded considerably below the initial maximum tensile stress. The final loading in pure compression (run 4) on specimen 5 shows a Bauschinger effect relative to run 3. The second loading on specimen 6 was at a ratio $\sigma/\tau \approx -3$. (See fig. 13.) The third and fourth loadings were in reversed torsion. Note the sharp bend in the τ,γ_p curve of run 4.

L
7
6
9

Specimen 7.- In order to obtain some indication of the location of the initial yield surface for these thin-walled tube specimens, specimen 7 was loaded initially in pure torsion and then in pure tension. (See fig. 14.) In reference 3 it was shown that for 2024-T4 aluminum alloy an initial pure-shear loading does not affect the yield point in pure tension. If the validity of this result is assumed for the present specimens, the initial yield surface can be approximated from the first two loadings on specimen 7. Based on the experiments on this single specimen, it appears that the initial yield surface lies close to the Tresca (maximum shear stress) criterion. The maximum stress for run 2 (pure tension) was about 32 percent above the yield point as was the case for the initial (pure tension) loads on all previous specimens. The results of runs 2 and 3 on specimen 7 are assumed to define the Bauschinger effect in tension-compression for this material.

DISCUSSION

Results reported in references 4 and 5 strongly suggest that the loading point, once it moves outside the initial yield surface, carries an obtuse corner with it. Based on this idea the present test results lead to two interesting conjectures. First, it is noted that sharply bending stress-strain curves are obtained when a radial loading path follows the immediately preceding path and extends farther into the plastic range. This phenomenon occurs on specimen 1, run 2; specimen 2, run 3; specimen 3, run 5; specimen 4, run 3; and specimen 6, run 4. If

it is presumed that the preceding radial loading formed a corner in the yield surface, then these results suggest that a sharp bend in the stress-strain curve may be associated with loading through a corner. Second, it is noted that when a radial loading follows a previous loading path but with intervening loadings along significantly different paths, a smooth stress-strain curve results. The intervening loadings influence drastically the yield surface near the corner. The effect is to erase the corner and pull the yield surface back toward and sometimes inside its original location. This behavior is illustrated by specimen 2, run 5; specimen 3, run 3; specimen 4, run 5; and specimen 5, run 3.

Not enough tests have been carried out in the neighborhood of the positive σ-axis to outline precisely the shape of the yield surface there. The conjectured shape shown in figure 7 is based to some extent on the results of references 4 and 5. As mentioned previously, reference 3 shows that initial pure-shear loading does not influence the yield point in pure tension; in the present investigation it is found that the initial pure-tensile stress does not influence the yield point in pure shear.

L
7
6
9

CONCLUDING REMARKS

Seven thin-walled tubes of 2014-T4 aluminum alloy were tested in combined tension or compression and torsion to determine the secondary yield surface in the normal-stress—shear-stress plane formed by initial loading in pure tension. This loading distorts the initial yield surface in the vicinity of the positive normal-stress (tension) axis but leaves it practically undistorted in the vicinity of the shear-stress axis. The elastic limit in compression is significantly reduced by the initial tensile load (Bauschinger effect).

The results indicate that a local peculiarity, perhaps a corner, is formed in the yield surface at a point of maximum radial loading. If the next loading is a radial loading through that point, a sharp bend occurs in the stress-strain curve. Intervening loads along different radial paths are found to influence drastically the yield surface in the vicinity of the corner, generally by pulling the yield surface back toward and sometimes inside its original location; and on subsequent loading through such a point, the resulting stress-strain curve is smooth.

Langley Research Center,
National Aeronautics and Space Administration,
Langley Field, Va., March 15, 1960.

REFERENCES

1. Hill, R.: The Mathematical Theory of Plasticity. The Clarendon Press (Oxford), 1950, pp. 15-23.

2. Batdorf, S. B., and Budiansky, Bernard: A Mathematical Theory of Plasticity Based on the Concept of Slip. NACA TN 1871, 1949.

3. Naghdi, P. M., Essenburg, F., and Koff, W.: An Experimental Study of Initial and Subsequent Yield Surfaces in Plasticity. Jour. Appl. Mech., vol. 25, no. 2, June 1958, pp. 201-209.

4. Phillips, Aris, and Gray, George A.: Experimental Determination of Corners in the Yield Surface. Tech. Rep. No. 5 (Contract Nonr-609(12)), Dept. Civil Eng., Yale Univ., Dec. 1958.

5. Phillips, Aris: Pointed Vertices in the Yield Surface. Tech. Rep. No. 7 (Contract Nonr-609(12)), Dept. Civil Eng., Yale Univ., Sept. 1959.

6. Budiansky, Bernard, Dow, Norris F., Peters, Roger W., and Shepherd, Roland P.: Experimental Studies of Polyaxial Stress-Strain Laws of Plasticity. Proc. First U.S. Nat. Cong. Appl. Mech. (Chicago, Ill., 1951), A.S.M.E., 1952, pp. 503-512.

L
7
6
9

TABLE I.- LOADING PROGRAM

Loading paths	Specimen	λ	Run	Type of loading	Date of test	Stress-strain data in figure -
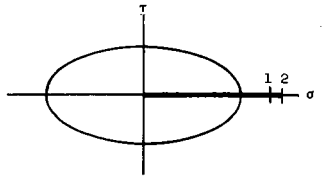	1	1.031	1 2	Pure tension	4-18-58	8
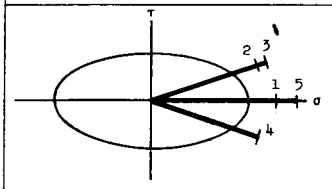	2	0.956	1 2 3 4 5	Pure tension Combined tension and torsion Combined tension and torsion Combined tension and reversed torsion Pure tension	9-10-58 9-11-58 9-11-58 9-11-58 9-11-58	9
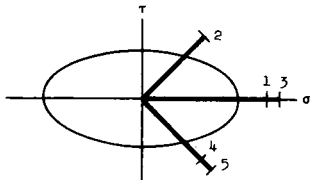	3	1.007	1 2 3 4 5	Pure tension Combined tension and torsion Pure tension Combined tension and reversed torsion Combined tension and reversed torsion	9-18-58 9-19-58 9-19-58 9-19-58 9-19-58	10
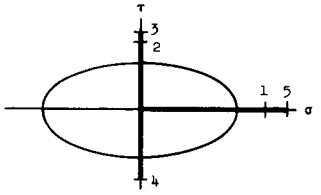	4	1.007	1 2 3 4 5	Pure tension Pure torsion Pure torsion Reversed torsion Pure tension	10-7-58	11
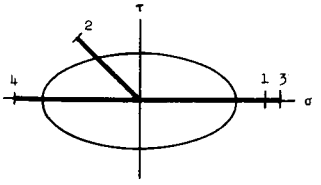	5	1.018	1 2 3 4	Pure tension Combined compression and torsion Pure tension Pure compression	12-5-58 12-8-58 12-8-58 12-8-58	12
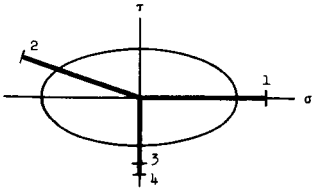	6	1.015	1 2 3 4	Pure tension Combined compression and torsion Reversed torsion Reversed torsion	12-18-58 12-19-58 12-19-58 12-19-58	13
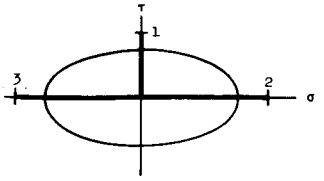	7	1.051	1 2 3	Pure torsion Pure tension Pure compression	1-16-59	14

L-769

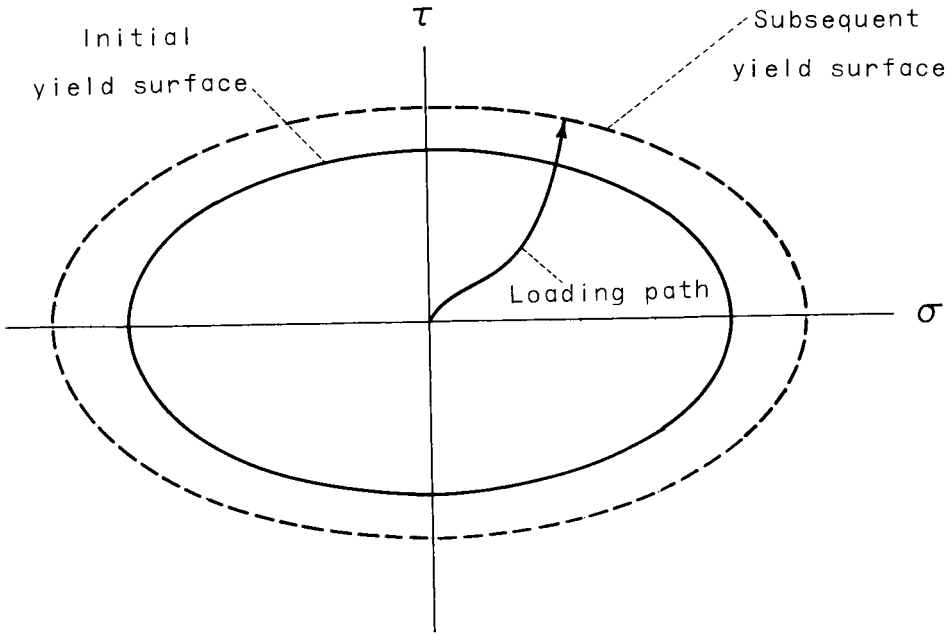

(a) J_2, or Von Mises flow theory.

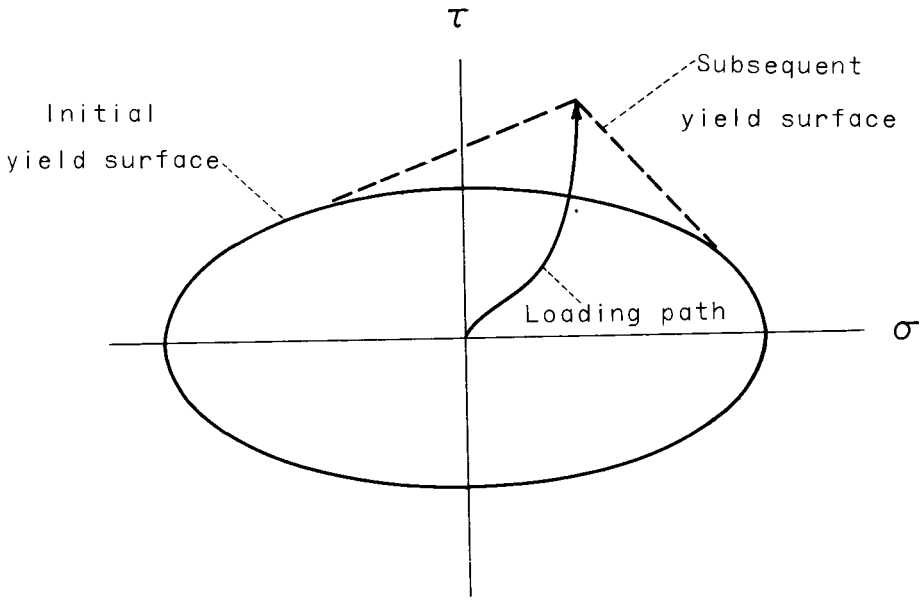

(b) Slip theory of Batdorf and Budiansky.

Figure 1.- Changes in yield surface predicted by two theories of plasticity.

L-169

L-769

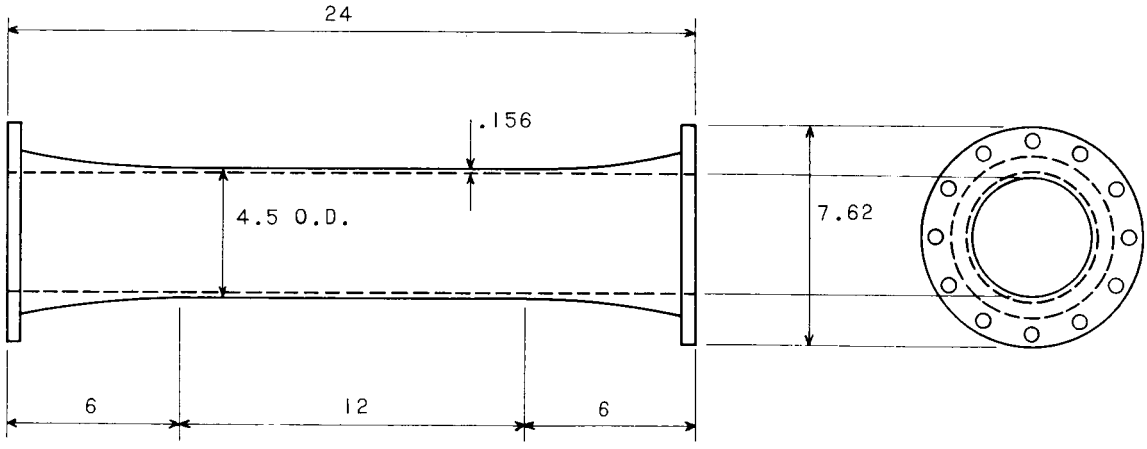

Figure 2.- Thin-walled tube specimen. All dimensions in inches.

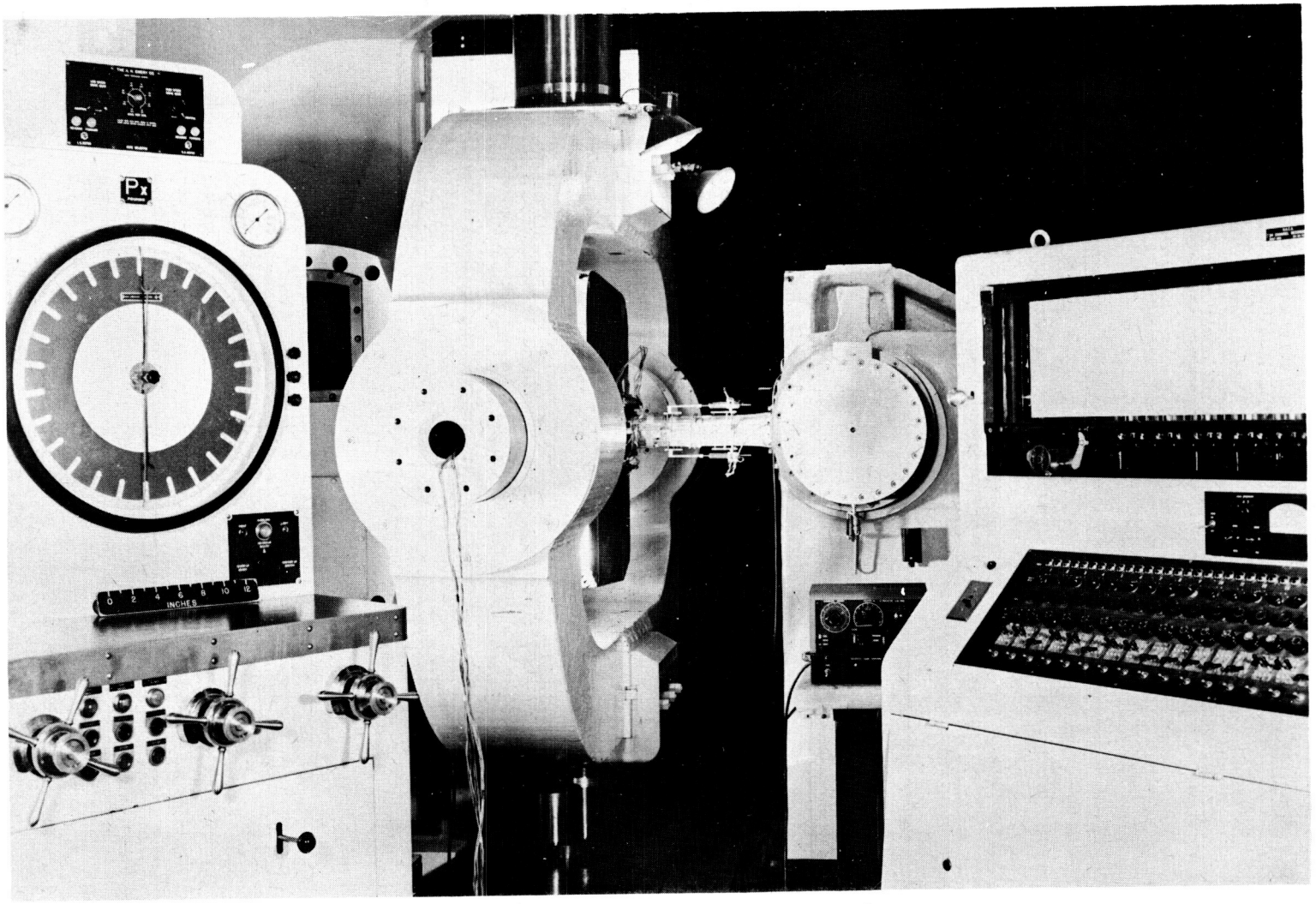

L-58-1943

Figure 3.- Combined load testing machine with a thin-walled tube specimen.

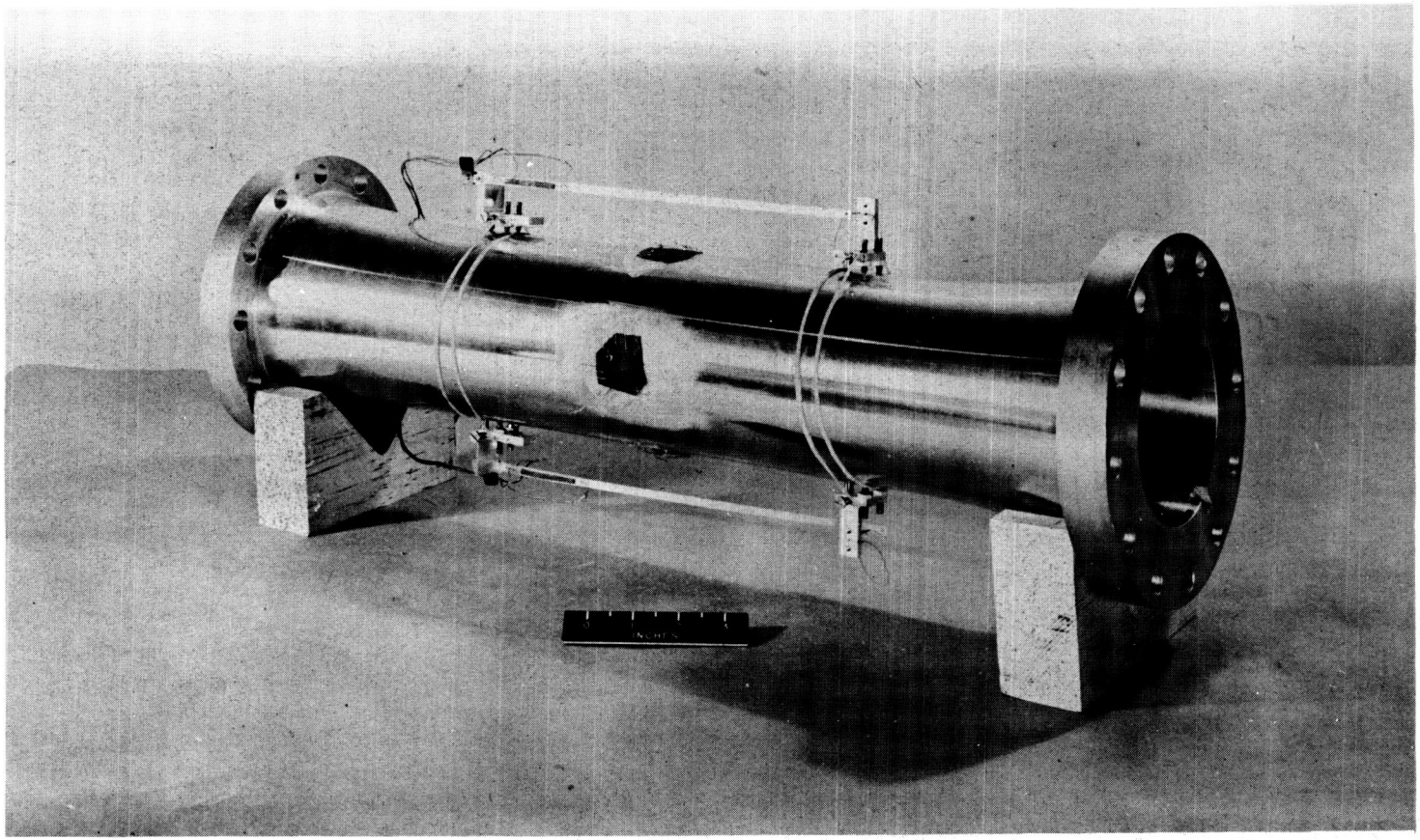

L-67728

Figure 4.- Twist gages and electrical-resistance strain rosettes mounted on a thin-walled tube specimen.

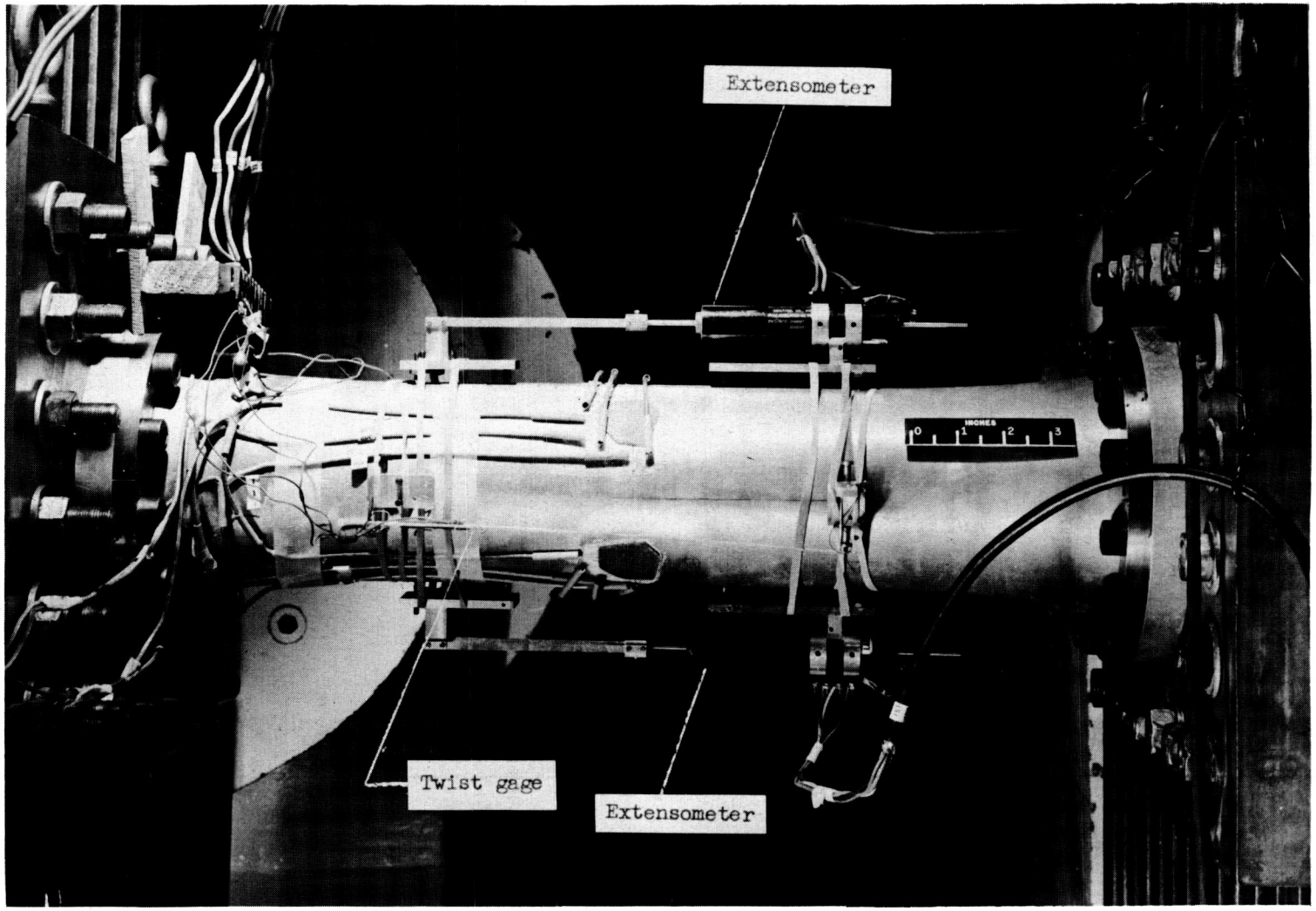

L-58-1944.1

Figure 5.- Completely instrumented thin-walled tube specimen mounted in combined load testing machine.

L-769

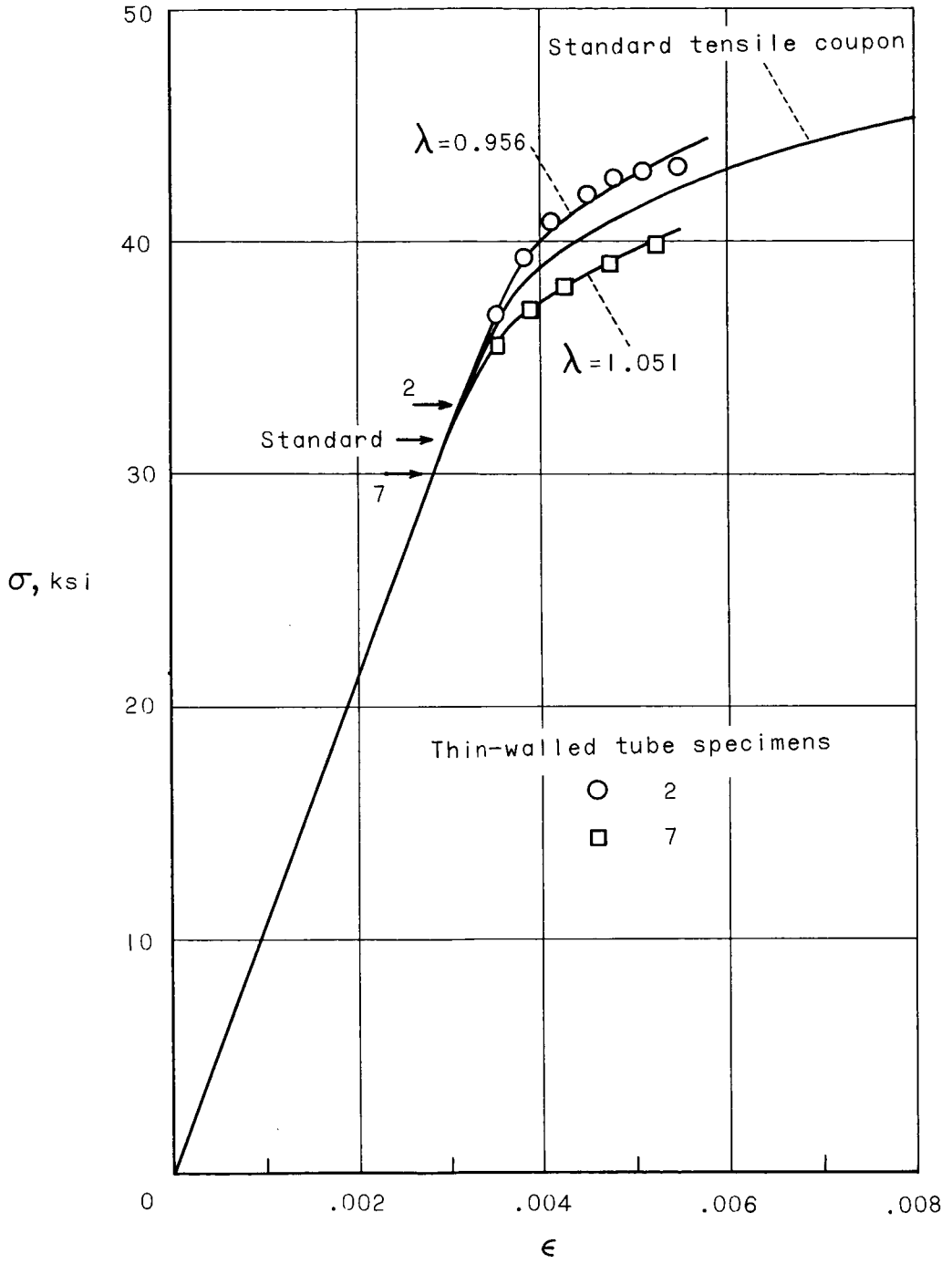

Figure 6.- Comparison between tensile stress-strain curves obtained from two thin-walled tube specimens and curves obtained from a standard stress-strain coupon by use of the relation $\epsilon_p = f(\lambda\sigma)$. Arrows denote yield points.

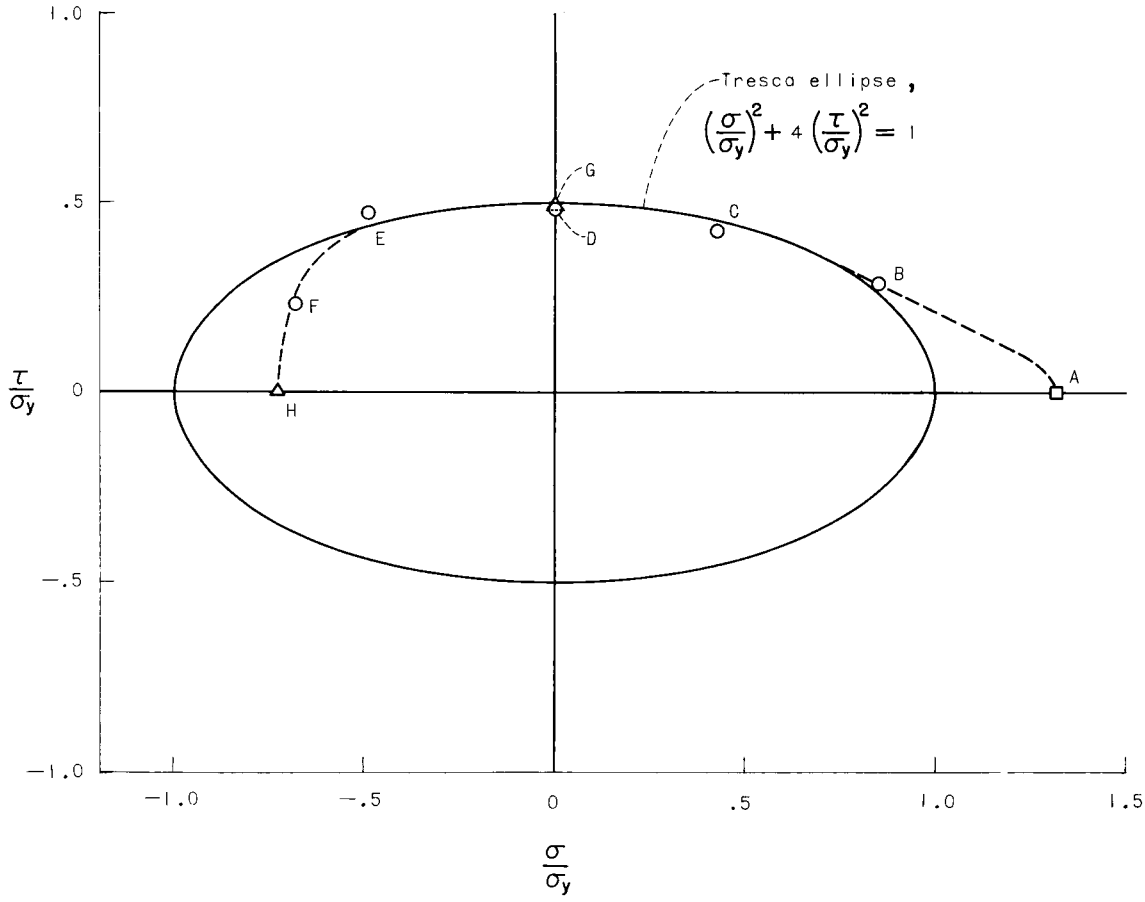

Figure 7.- Initial and secondary yield surfaces in σ,τ plane. Dashed curve shows secondary yield surface.

L-799

L-769

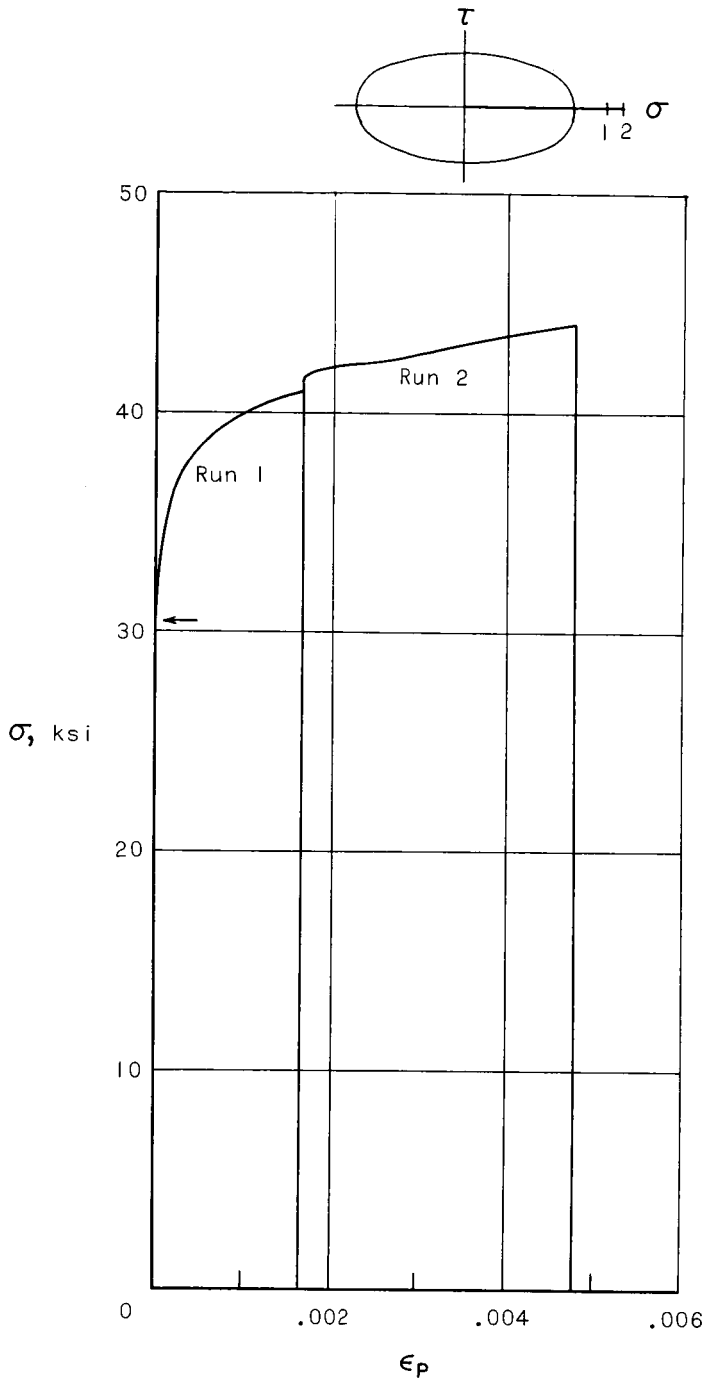

Figure 8.- Normal-stress—plastic-strain curves for specimen 1. Arrow denotes yield point.

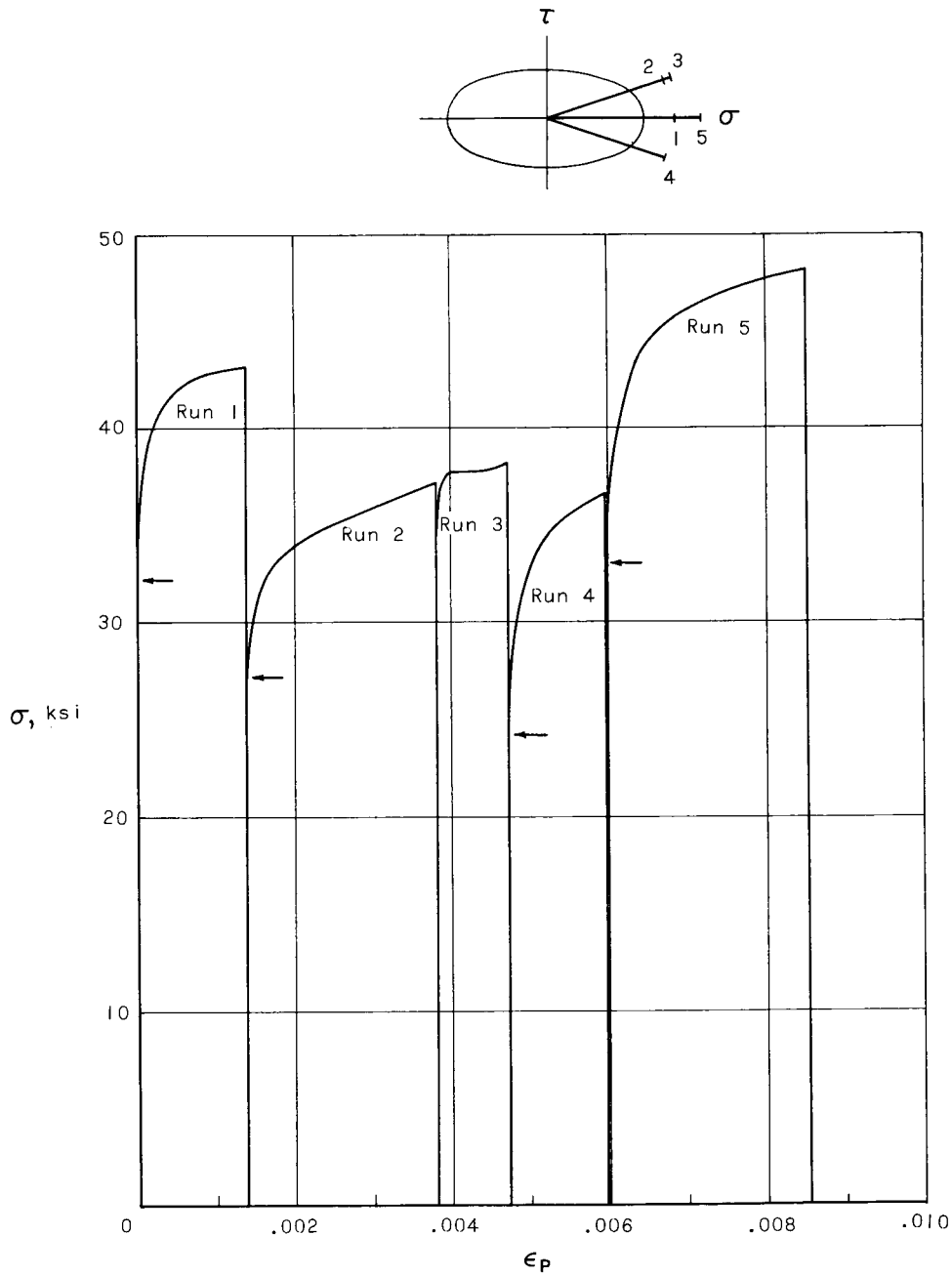

(a) Normal-stress—strain curves.

Figure 9.- Stress—plastic-strain curves for specimen 2. Arrows denote yield points.

L-769

L-769

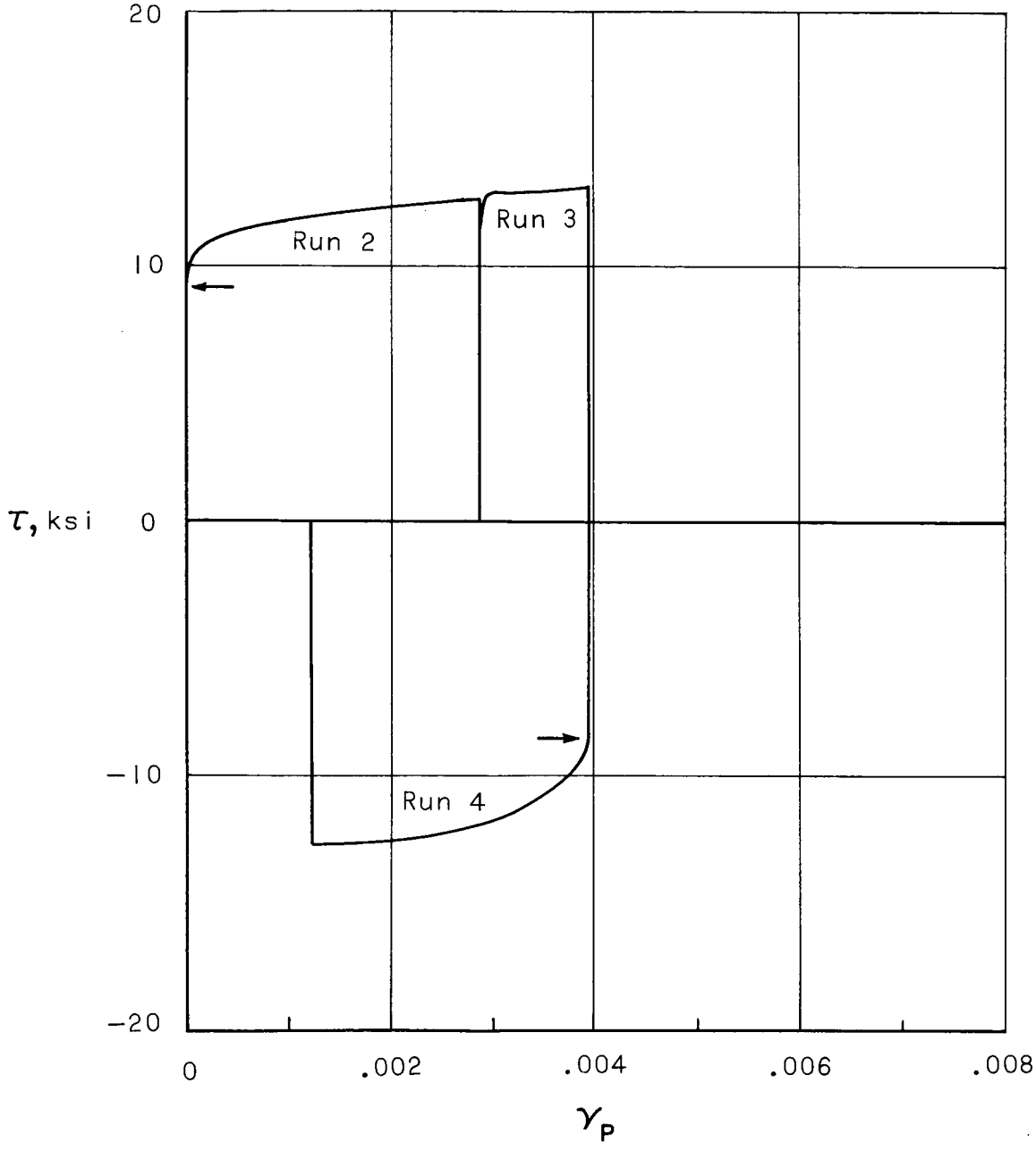

(b) Shear-stress—strain curves.

Figure 9.- Concluded.

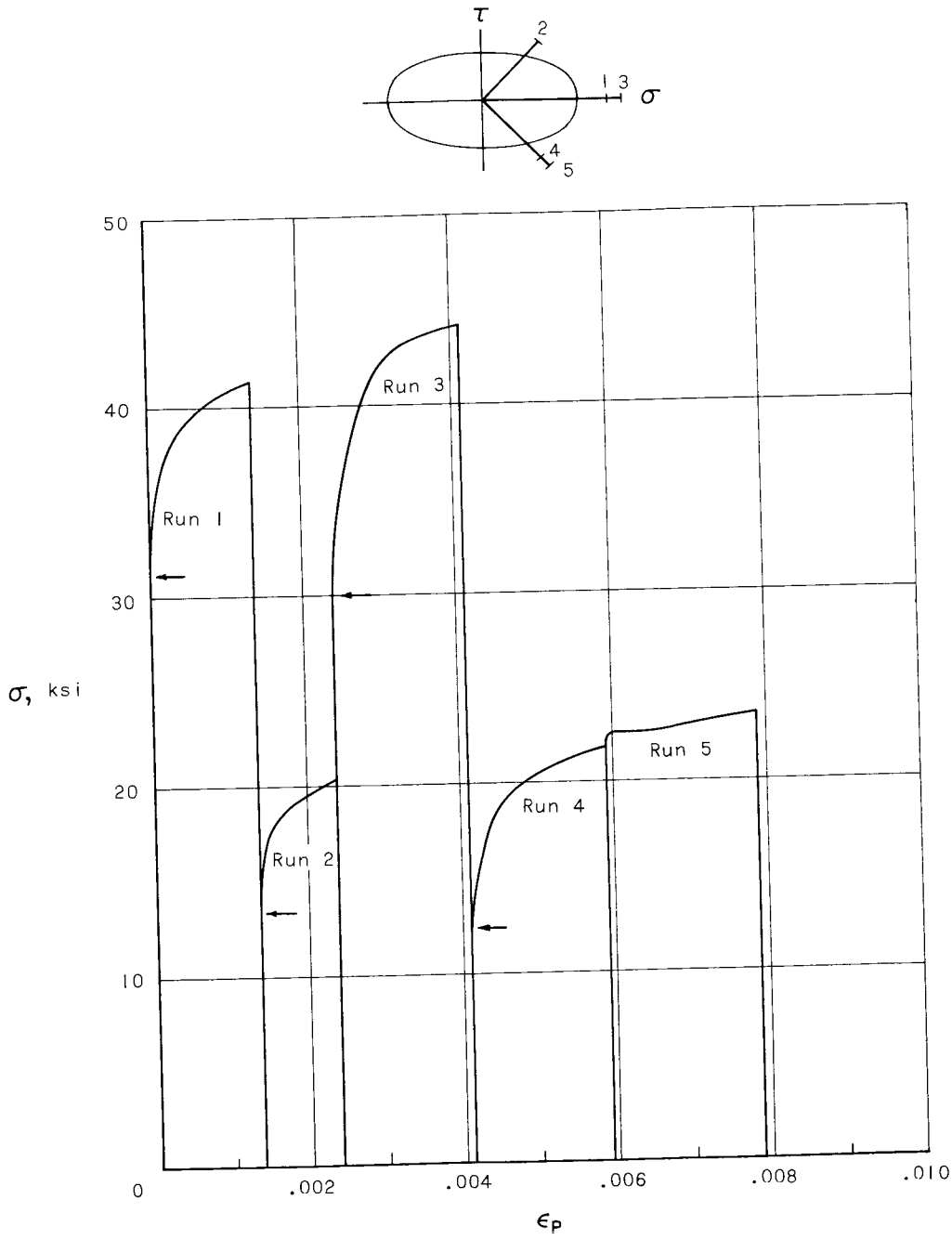

(a) Normal-stress—strain curves.

Figure 10.- Stress—plastic-strain curves for specimen 3. Arrows denote yield points.

L-769

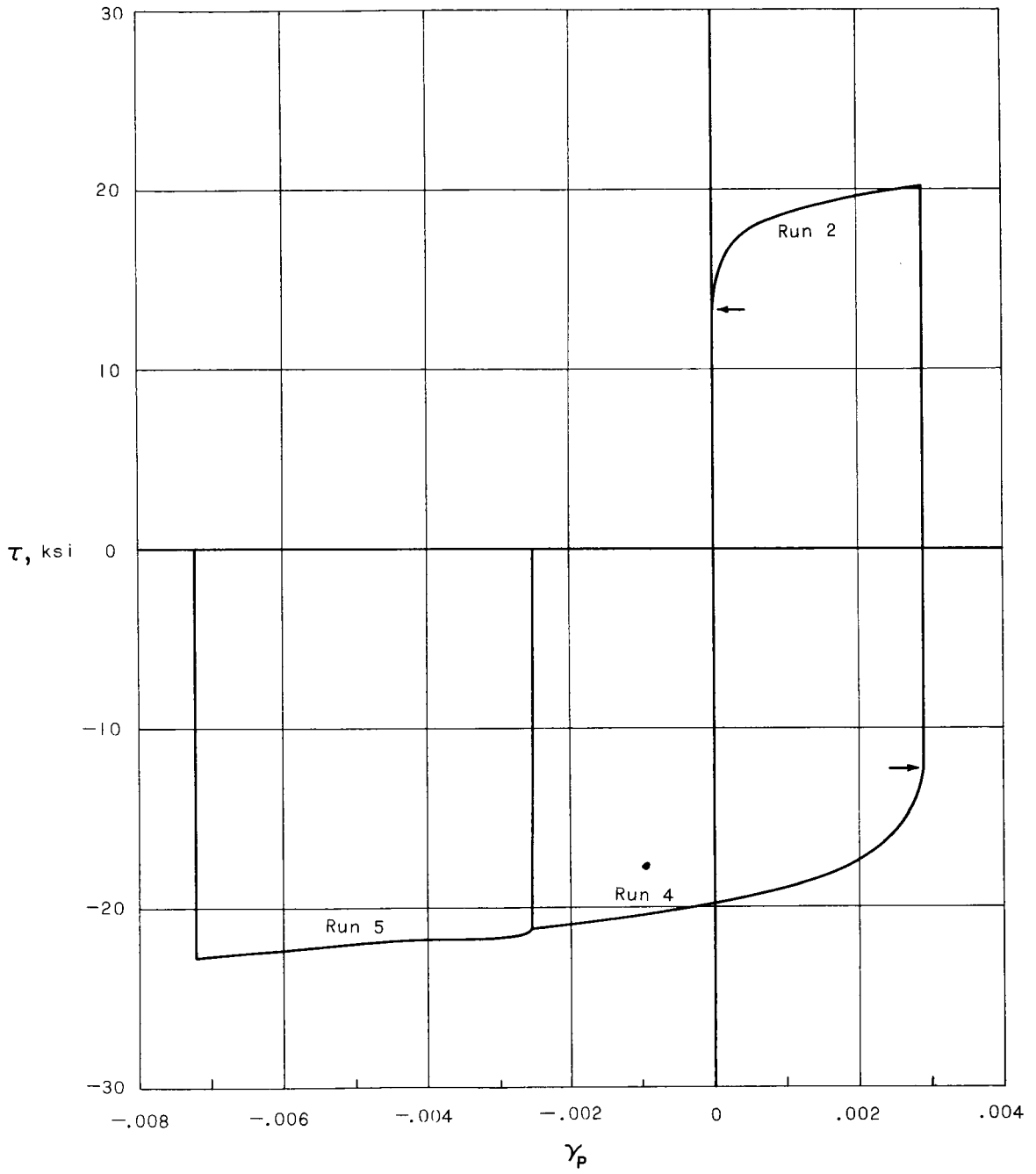

(b) Shear-stress—strain curves.

Figure 10.- Concluded.

L-769

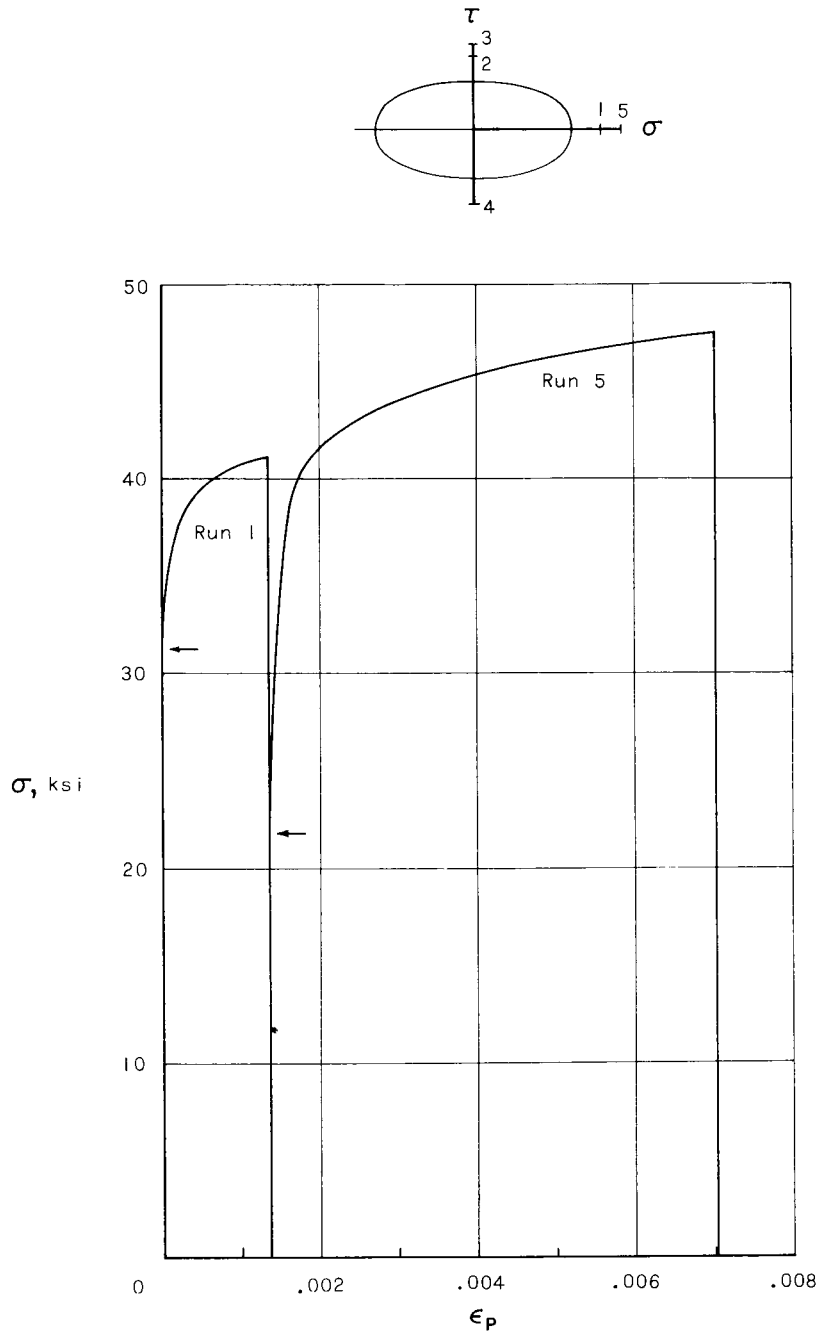

(a) Normal-stress—strain curves.

Figure 11.- Stress—plastic-strain curves for specimen 4. Arrows denote yield points.

L-769

L-769

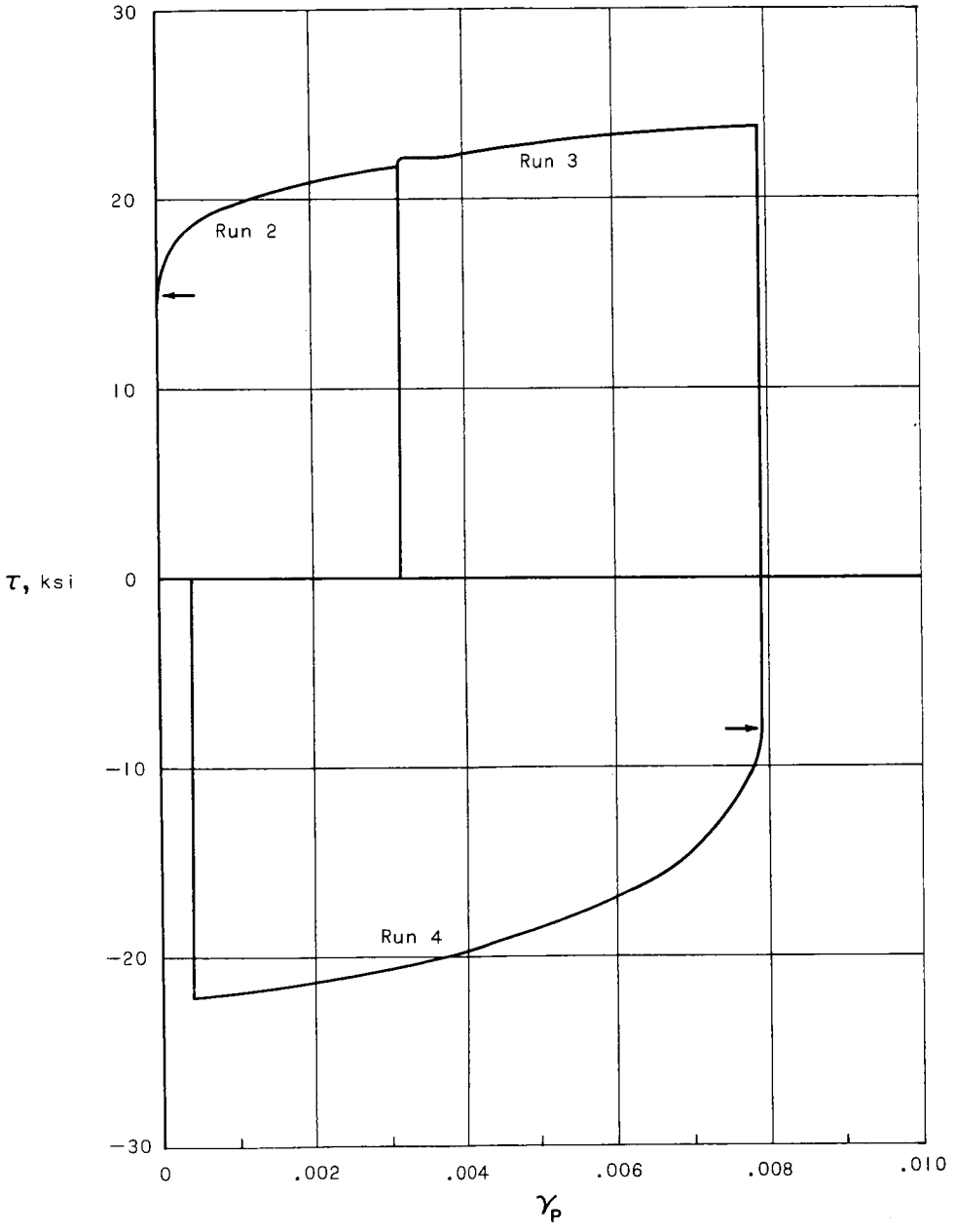

(b) Shear-stress—strain curves.

Figure 11.- Concluded.

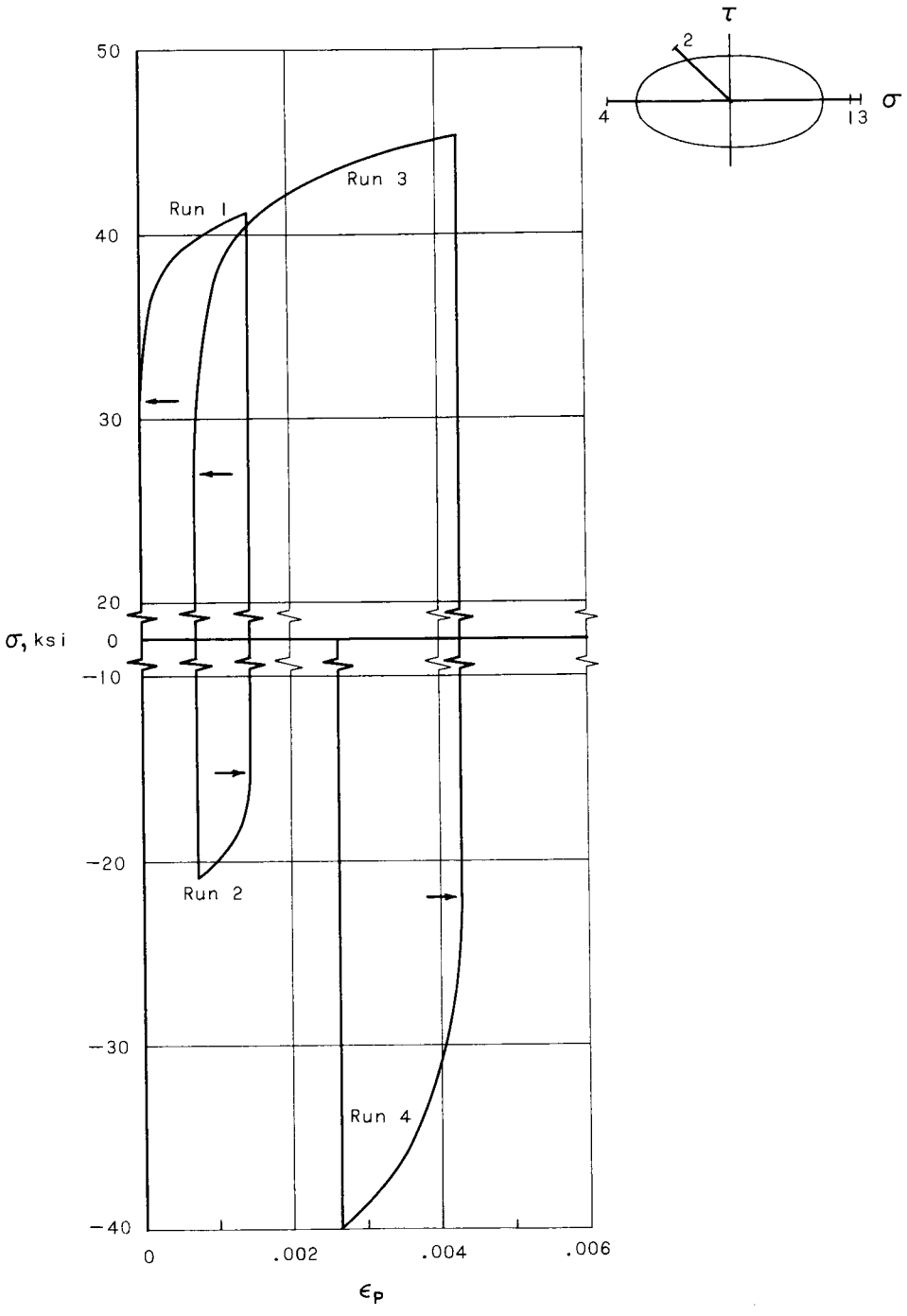

(a) Normal-stress—strain curves.

Figure 12.- Stress—plastic-strain curves for specimen 5. Arrows denote yield points.

L-769

L-769

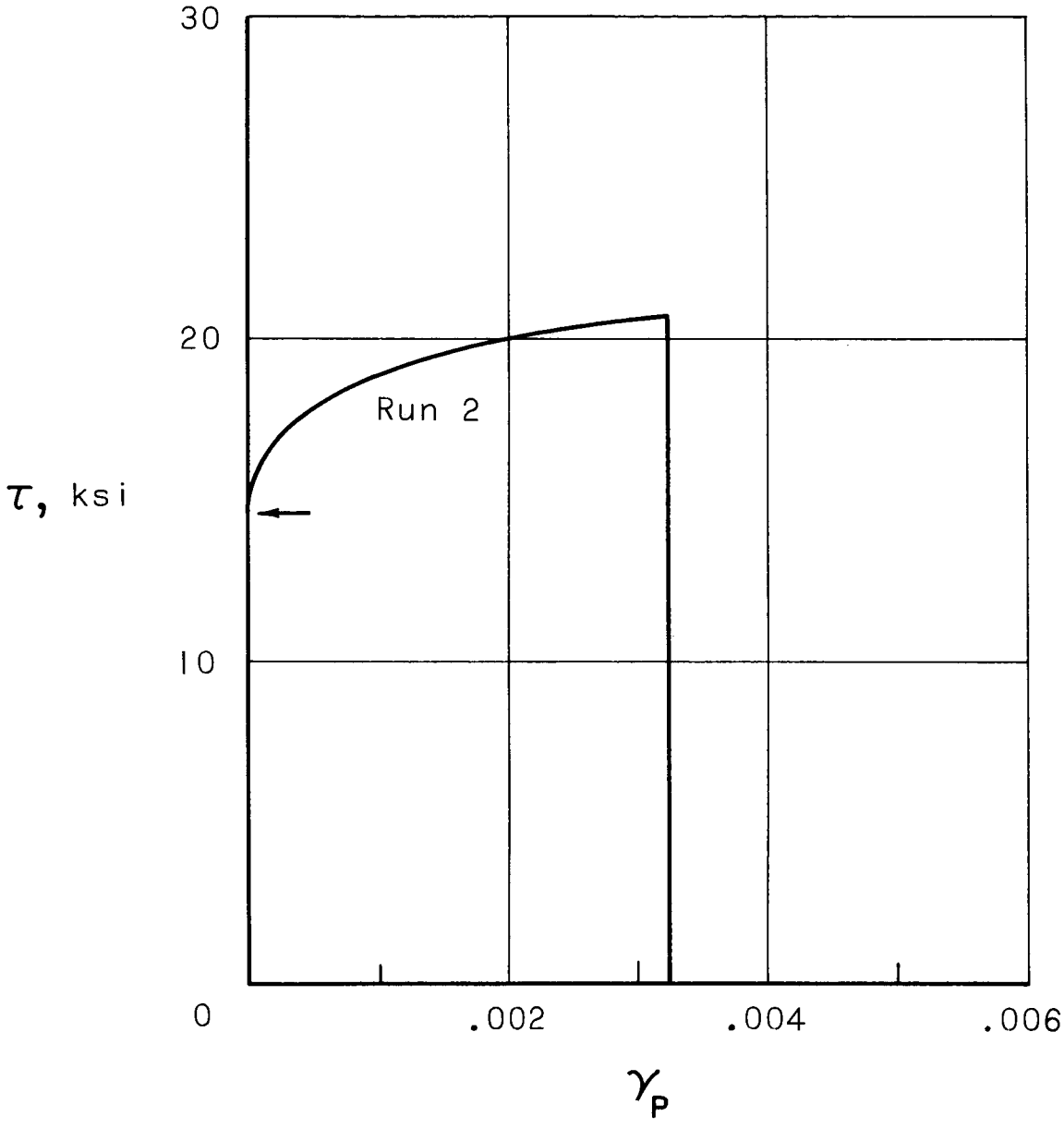

(b) Shear-stress—strain curves.

Figure 12.- Concluded.

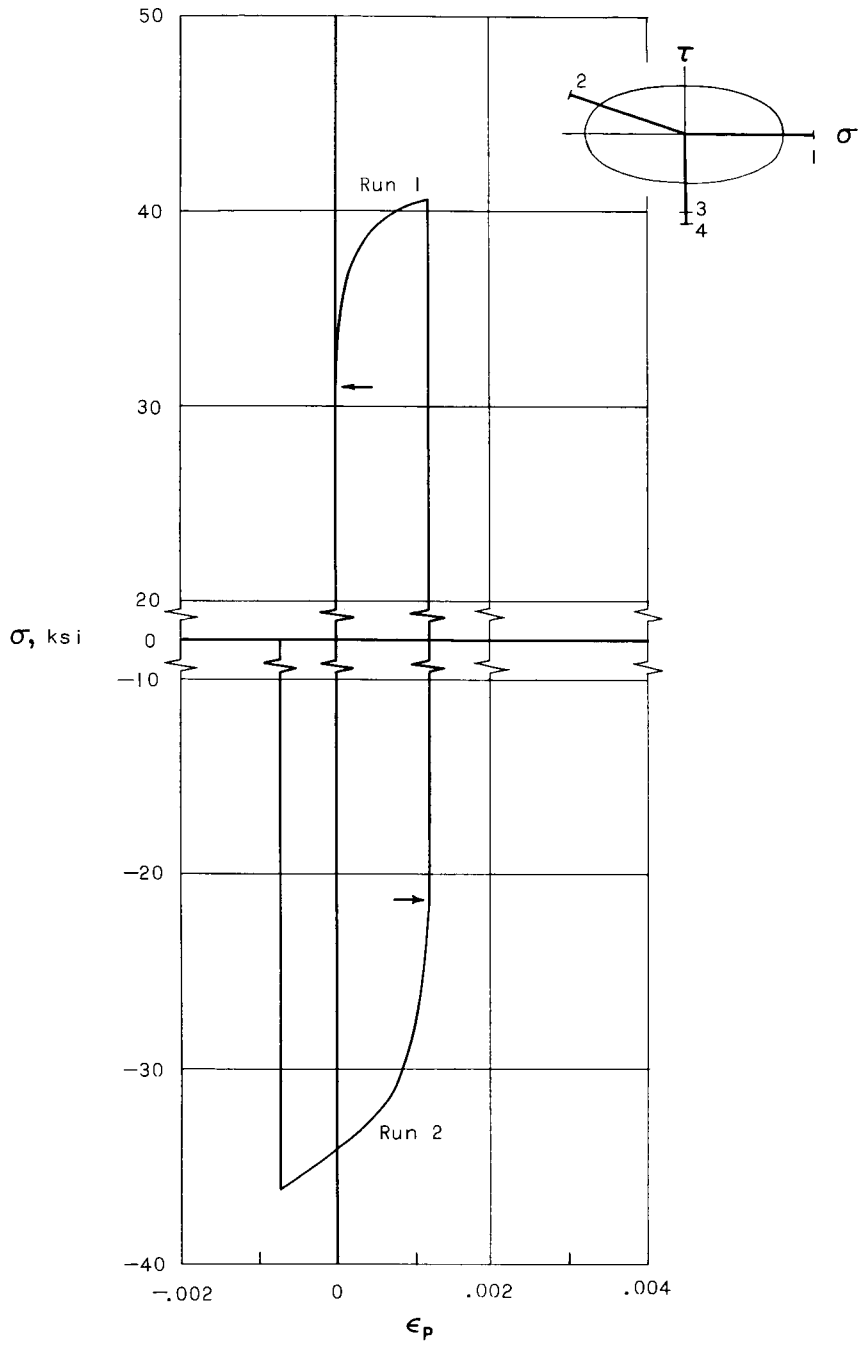

(a) Normal-stress—strain curves.

Figure 13.- Stress—plastic-strain curves for specimen 6. Arrows denote yield points.

L-769

L-769

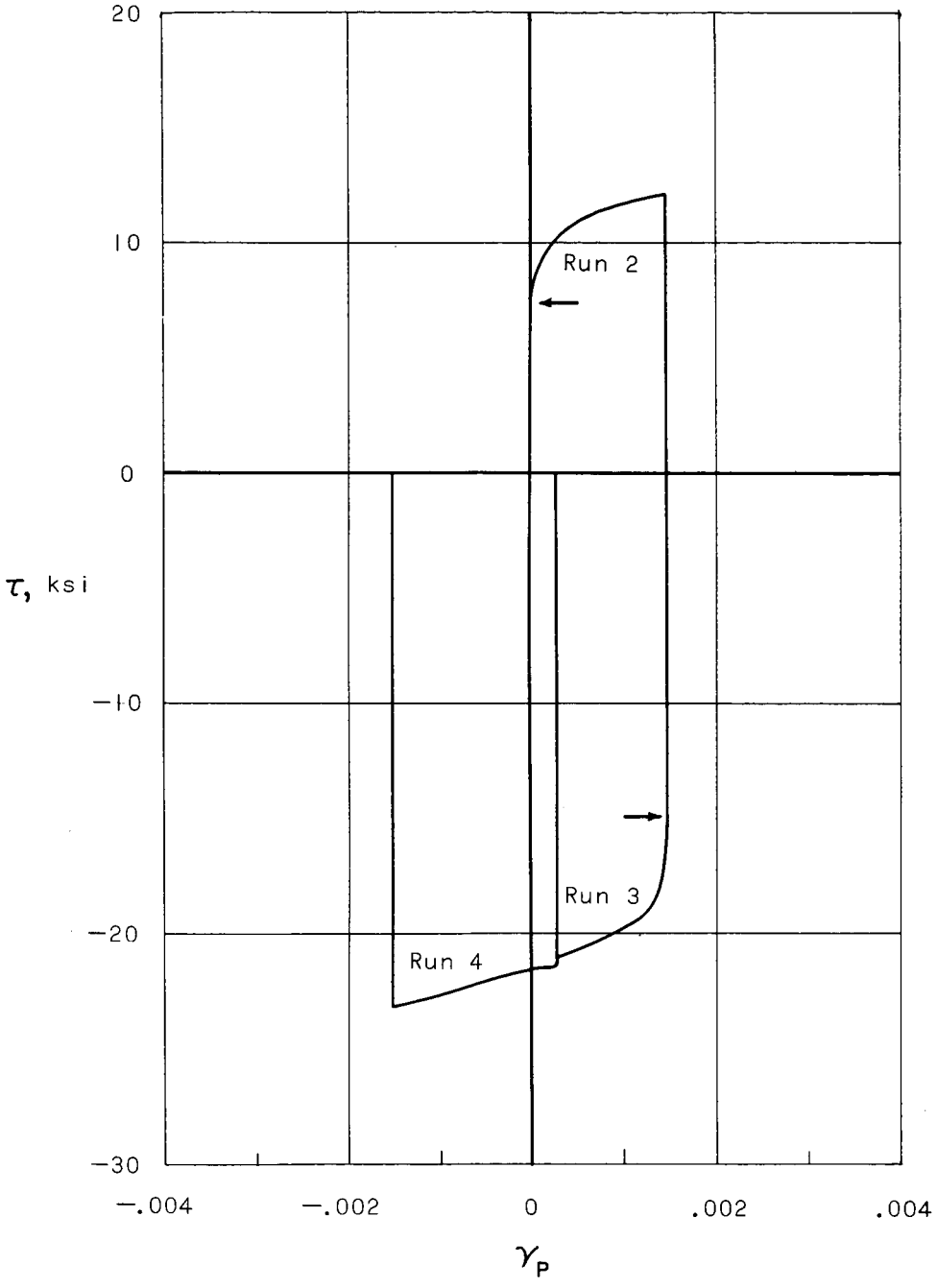

(b) Shear-stress—strain curves.

Figure 13.- Concluded.

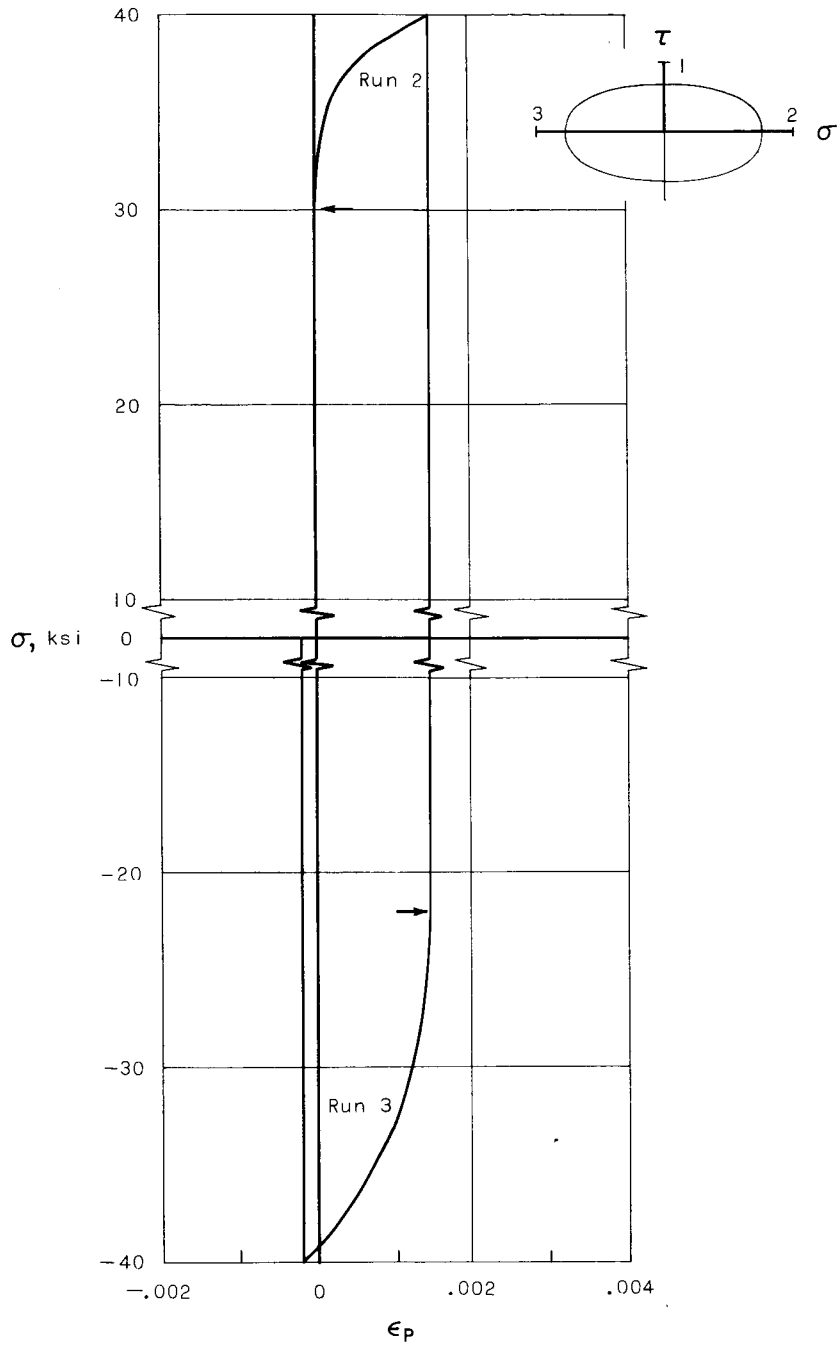

(a) Normal-stress—strain curves.

Figure 14.- Stress—plastic-strain curves for specimen 7. Arrows denote yield points.

L-769

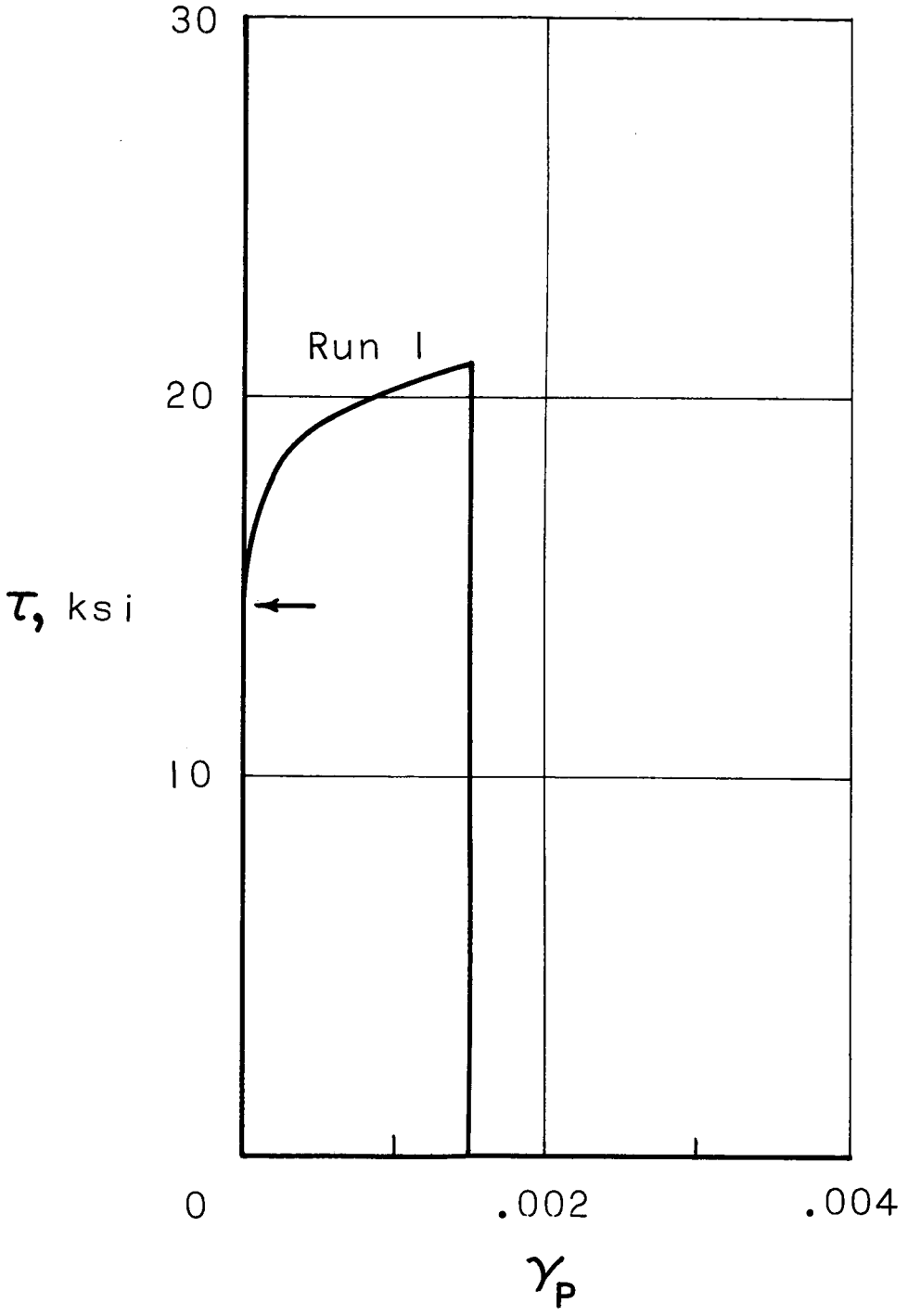

(b) Shear-stress—strain curves.

Figure 14.- Concluded.